JOURNAL OF MATERIALS SCIENCE: MATERIALS IN ELECTRONICS, 4 (1993) 215–224

Thermodynamic properties of AsH_3 and its subhydrides

A. S. JORDAN
AT&T Bell Laboratories, Murray Hill, New Jersey 07974, USA
A. ROBERTSON, JR
Engineering Research Center, Princeton, New Jersey 08540, USA

The thermodynamic properties of AsH_3 and its subhydrides AsH and AsH_2 have been evaluated from critically assessed or estimated spectroscopic data. The calculation of thermodynamic functions (free-energy function, entropy, enthalpy, and heat capacity) is based on statistical thermodynamics. For the first time, for all three species a complete set of these functions has been generated between 0 and 1600 K in tabular form. A combination of the free-energy functions with the standard enthalpies of formation of hydrides (derived from the photoionization mass-spectrometric bond energy values of Berkowitz) permits the determination of the gas phase composition in the pyrolysis of AsH_3 during the MOMBE (CBE), HS-MBE, or MOCVD growth of III–V epitaxial layers that include As. Using a free-energy minimization technique, the equilibrium concentrations of AsH, AsH_2, AsH_3, As, As_2, As_4, H and H_2 have been obtained at 1.013, 3.039×10^3 and 1.013×10^5 Pa (1 atm) in the temperature range between 800 and 1500 K. In the case of MOMBE, under equilibrium conditions in the hydrate cracker, the removal of carbon-containing radicals or oxygen is facilitated by atomic H and AsH with partial pressures of $\sim 3.33 \times 10^{-4}$ and 1.87×10^{-5} Pa, respectively, at 1300 K. In contrast, in low pressure MOCVD the species AsH and AsH_2 are equally prominent, while in atmospheric pressure MOCVD the dominant subhydride is AsH_2.

1. Introduction

Arsine and phosphine are the most widely used sources of arsenic and phosphorus in the epitaxial growth of III–V compound semiconductor films by metal-organic chemical vapor deposition (MOCVD), hydride-source molecular beam epitaxy (HS-MBE), and metal-organic MBE (MOMBE also known as CBE). In MOCVD the pyrolysis of arsine and phosphine occurs in the presence of a complex mixture of chemical species by both heterogeneous and homogeneous pathways [1]. In contrast, in the molecular beam technologies the hydrides are cracked in a high-temperature effusion cell before impinging on the surface of the wafer, allowing control of the hydride pyrolysis independent of the substrate temperature. For all of these advanced techniques an understanding of the distribution of As and/or P as well as hydrogen-containing species incident at the epitaxial growth front is essential in optimizing and controlling the growth processes with respect to film stoichiometry, growth rate and purity.

Although chemical kinetics plays a significant role in effecting the concentration of various species, a thermodynamic analysis of the pyrolysis has intrinsic merit. First, the rate of approach of a chemical system toward an equilibrium state is governed by chemical kinetics while the nature of the equilibrium state (concentration of reactants and products) is given by thermodynamics. More specifically, the nature of the equilibrium state is independent of any mechanistic path to reach it and is solely a function of the species and their free energies. Second, for any mechanism, a detailed balance of all the forward and reverse reactions produces a rate law in which only two parameters from a set of three (forward and reverse rates, equilibrium constant) are independent. Thus, a thermodynamic determination of an equilibrium constant can be used to calculate a rate constant for any mechanistic step in which one of the rate constants is known.

Furthermore, at high temperatures, long reaction residence times, or when using catalysts, kinetic limitations may become minimal and there is a need to understand the equilibrium state. When complete thermodynamic data for expected transient species such as AsH, AsH_2 and H are available, it is possible to calculate their equilibrium concentrations and assess their potential impact on growth chemistry. For example, a knowledge of concentrations facilitates the identification of the species (i.e. AsH, AsH_2 or H) responsible for reducing carbon incorporation in AsH_3–based MOCVD and MOMBE. Thermodynamics may provide an important benchmark in gauging kinetic effects and supports process optimization for epitaxial growth.

There is a complete set of thermodynamic data for phosphine and its subhydrides (PH, PH_2) in a standard compilation [2]. In another source, the NBS

0957–4522 © *1993 Chapman & Hall*

Tables [3], only the properties of AsH_3 at 298 K are included. However, the available values for AsH and AsH_2 are sparse [4]. The major objective of this paper is to evaluate in detail thermodynamic functions of AsH_3 and its subhydrides over a wide temperature range. In calculating the free-energy functions, entropies, enthalpies and heat capacities, the methods of statistical thermodynamics were employed in conjunction with critically assessed or estimated spectroscopic data. In addition, based on the recent photoionization mass spectrometric measurements of Berkowitz which give the bond energies of As hydrides [5], we determined the standard enthalpics of formation. Using a free-energy minimization technique, the new data were applied to the thermal decomposition of AsH_3 in order to obtain the equilibrium concentrations of As, As_2, As_4, AsH, AsH_2, AsH_3, H, and H_2 at selected total pressures as a function of temperature. Finally, important conclusions are drawn from the calculated results are compared with and/or applied to some experimental data in MOMBE (HS-MBE), low pressure MOCVD and atmospheric pressure MOCVD.

2. Evaluation of properties by statistical thermodynamics

The thermodynamic properties of gaseous molecules as a function of temperature can be readily calculated from statistical mechanics provided the structures and vibrational frequencies are known from spectroscopic data [2, 6]. The translational rotational, vibrational, and electronic contributions to the entropy, S°, and free-energy function, FEF, are given below. Similar formulae for the heat capacity, C_p°, and enthalpy difference, $H^\circ - H_0^\circ$, are also readily available from the cited references [2, 6].

2.1. Translational contribution

In the ideal gas standard state at 1.013×10^5 Pa (1 atm) the translational contributions to the entropy (S_{tr}°) and free-energy function (FEF_{tr}) are given by

$$S_{tr}^\circ[\text{cal deg}^{-1}\ \text{mol}^{-1}] = R(1.5 \ln M + 2.5 \ln T) - 2.315 \quad (1)$$

$$FEF_{tr}[\text{cal deg}^{-1}\ \text{mol}^{-1}] = -\left[\frac{F^\circ - H_0^\circ}{T}\right]_{tr} = R(1.5 \ln M + 2.5 \ln T) - 7.283 \quad (2)$$

where F°, H_0°, M, T and R, respectively, denote the free energy, enthalpy at 0 K, molecular weight, absolute temperature and the gas constant. In Table I, the translational contributions to the thermodynamic properties of AsH, AsH_2 and AsH_3 at 298, 1000 and 1500 K are summarized.

2.2. Rotational contribution

In evaluating the rotational contribution to the entropy, S_{rot}°, free-energy function, FEF_{rot}, etc., one has to differentiate between diatomic (AsH) and polyatomic (AsH_2, AsH_3) molecules. In the rigid rotor approximation S_{rot}° and FEF_{rot} for a diatomic molecule are given by [2, 6]

$$S_{rot}^\circ = R\left(1 - \ln y - \ln \sigma - \frac{y^2}{90} - \cdots\right) \quad (3)$$

and

$$FEF_{rot} = -\left[\frac{(F^\circ - H_0^\circ)}{T}\right]_{rot} = R\left(-\ln y - \ln \sigma + \frac{y}{3} + \frac{y^2}{90} + \cdots\right) \quad (4)$$

where σ is the symmetry number and y is a dimensionless quantity that can be expressed in terms of the spectroscopic constant (B) or the moment of inertia (I) in the forms

$$y = \frac{hcB}{kT} = \frac{h^2}{8\pi^2 IkT} \quad (5)$$

where h, c, and k are Planck's constant, the speed of light, and the Boltzmann constant, respectively.

The symmetry number for AsH, AsH_2 and AsH_3, respectively, is 1, 2, and 3. The moment of inertia of the molecule is taken about an axis through the centre of gravity and perpendicular to the axis on which the atoms reside. For a diatomic molecule such as AsH the moment of inertia is

$$I = m_1(1 - q)^2 + m_5 q^2 \quad (6)$$

where m_1 and m_5 are the masses of hydrogen and the group V atom, respectively. The quantity q is related to the masses and the equilibrium interatomic distance, l, according to

$$q = \frac{m_1}{m_1 + m_5} l \quad (7)$$

In Table I are listed the rotational contributions to the entropy, FEF, enthalpy, and heat capacity of AsH at 298, 1000, and 1500 K. The relevant structural information [7] is provided in Table II.

In the case of polyatomic molecules the rotational entropy and FEF in the 'high temperature approximation' take the following forms [6]:

$$S_{rot}^\circ = R[0.5 \ln(D \times 10^{117}) + 1.5 \ln T - \ln \sigma] - 0.033 \quad (8)$$

$$FEF_{rot} = -\left[\frac{F^\circ - H_0^\circ}{T}\right]_{rot} = R[0.5 \ln(D \times 10^{117}) + 1.5 \ln T - \ln \sigma] - 3.014 \quad (9)$$

where D represents a determinant that can be expanded to

$$D = I_x I_y I_z - 2I_{xy} I_{yz} I_{xz} - I_x I_{yz}^2 - I_y I_{xz}^2 - I_z I_{xy}^2 \quad (10)$$

with the moments and products of inertia, if the origin of the cartesian axes coincide with the centre of mass, given by

$$I_x = \sum_i m_i(y_i^2 + z_i^2), \quad I_{xy} = \sum_i m_i x_i y_i \quad (11)$$

Similar expressions can be readily defined for the other quantities in Equation 10.

For AsH_2 it can be easily shown that D is of the form

$$D = I_x I_y I_z, \quad I_z = I_x + I_y$$

where

$$I_x = 2m_1(l \sin \alpha/2)^2$$

$$I_y = 2m_1(l \cos \alpha/2 - q)^2 + m_5 q^2$$

$$q = \frac{2\, l m_1 \cos \alpha/2}{2m_1 + m_5}$$

The quantities l and α are the equilibrium AsH bond length and As–H_2 bond angle, respectively.

For AsH_3, a pyramidal molecule, the calculation is more cumbersome. After some algebraic operations we find for D

$$D = I_x I_y I_z$$

where

$$I_x = m_1\left(3q^2 + \frac{\phi^2}{2}\right) + m_5(h - q)^2$$

$$I_y = I_x$$

$$I_z = m_1 \phi^2$$

and

$$h = l(1 - 4/3 \sin^2 \alpha/2)^{1/2}$$

TABLE Ia Contributions to the thermodynamic functions of AsH (g)

Temperature (K)	Contribution	S° (cal mol^{-1} deg^{-1})	FEF (cal mol^{-1} deg^{-1})[a]	$H^\circ - H_0^\circ$ (cal mol^{-1})	C_p° (cal mol^{-1} deg^{-1})
	tr	38.898	33.930	1481.3	4.968
	rot	8.648	6.684	585.6	1.987
298	vib	0.001	0.00009	0.3	0.009
	anh	0.011	0.005	1.6	0.011
	el	2.183	2.183	0	0
	Total	49.741	42.803	2068.7	6.975
	tr	44.910	39.942	4968.2	4.968
	rot	11.053	9.073	1980.3	1.987
1000	vib	0.418	0.103	315.0	0.991
	anh	0.053	0.022	31.6	0.090
	el	2.183	2.183	0	0
	Total	58.618	51.323	7295.1	8.036
	tr	46.925	41.957	7452.2	4.968
	rot	11.857	9.876	2974.0	1.987
1500	vib	0.917	0.291	937.9	1.442
	anh	0.105	0.040	96.3	0.170
	el	2.183	2.183	0	0
	Total	61.988	54.348	11460.3	8.567

[a] $FEF = -(F^\circ - H_0^\circ)/T$

TABLE Ib Contributions to the thermodynamic functions of AsH_2 (g)

Temperature (K)	Contribution	S° (cal mol^{-1} deg^{-1})	FEF (cal mol^{-1} deg^{-1})[a]	$H^\circ - H_0^\circ$ (cal mol^{-1})	C_p° (cal mol^{-1} deg^{-1})
	tr	38.937	33.969	1481.3	4.968
	rot	13.395	10.414	888.8	2.981
298	vib	0.112	0.020	27.5	0.440
	el	1.377	1.377	0	0
	Total	53.821	45.780	2397.5	8.389
	tr	44.950	39.982	4968.2	4.968
	rot	17.002	14.021	2980.9	2.981
1000	vib	2.318	0.776	1542.1	3.664
	el	1.377	1.377	0	0
	Total	65.648	56.157	9491.1	11.613
	tr	46.964	41.996	7452.2	4.968
	rot	18.211	15.230	4471.3	2.981
1500	vib	4.034	1.584	3675.5	4.725
	el	1.377	1.377	0	0
	Total	70.586	60.187	15599.0	12.674

[a] $FEF = -(F^\circ - H_0^\circ)/T$

TABLE Ic Contributions to the thermodynamic functions of AsH_3 (*g*)

Temperature (K)	Contribution	S° (cal mol^{-1} deg^{-1})	FEF (cal mol^{-1} deg^{-1})[a]	$H^\circ - H_0^\circ$ (cal mol^{-1})	C_p° (cal mol^{-1} deg^{-1})
	tr	38.976	34.008	1481.3	4.968
	rot	13.952	10.971	888.8	2.981
298	vib	0.324	0.057	79.5	1.262
	el	0	0	0	0
	Total	53.252	45.036	2449.5	9.211
	tr	44.989	40.021	4968.2	4.968
	rot	17.559	14.578	2980.9	2.981
1000	vib	5.632	1.989	3642.6	7.972
	el	0	0	0	0
	Total	68.180	56.588	11591.6	15.921
	tr	47.002	42.035	7452.2	4.968
	rot	18.769	15.788	4471.3	2.981
1500	vib	9.266	3.829	8155.0	9.819
	el	0	0	0	0
	Total	75.037	61.652	20078.5	17.768

[a] $FEF = -(F^\circ - H_0^\circ)/T$

TABLE II Structural data for AsH, AsH_2 and AsH_3

Formula	l(nm)	α (deg)	σ	g	$I \times 10^{-40}$ (g cm^2)	$D \times 10^{-120}$ (g^3 cm^6)
AsH	0.1528	180	1	3	3.86	
AsH_2	0.1521	90.7	2	2		111.63
AsH_3	0.1517	92.2	3	1		440.23

Atomic weights: As – 74.9216
(g-atom) H – 1.0079

$$q = \frac{m_5}{3m_1 + m_5} h$$

$$\phi = 2l \sin \alpha/2$$

The relevant structural information for AsH_2 and AsH_3 [7] are listed in Table II. In Table I are summarized the rotational contributions to the entropy, FEF, enthalpy and heat capacity of AsH_2 and AsH_3 at 298, 1000, and 1500 K.

2.3. Vibrational contribution

For harmonic vibrations the calculation of thermodynamic functions for gaseous molecules with n atoms ($n > 2$) is straightforward if the normal modes of vibrations are known from the infrared or Raman spectra. The formulae for the vibrational entropy, S_v°, and free-energy function are familiar from Einstein's treatment of the quantized harmonic oscillator [6]. Accordingly,

$$S_v^\circ = R \sum_{i=1}^{m} \left[\frac{u_i}{\exp(u_i) - 1} - \ln(1 - \exp(-u_i)) \right] \quad (12)$$

$$FEF_v = -\left[\frac{(F^\circ - H_0^\circ)}{T} \right]_v$$

$$= -R \sum_{i=1}^{m} \ln(1 - \exp(-u_i)) \quad (13)$$

where

$$u_i = \frac{h\nu_i}{kT} = \frac{hc\omega_i}{kT}$$

and the sum is over the $m = 3n - 6$ normal modes of vibration for a non-linear molecule. The symbols ν_i and ω_i represent the frequency in units of s^{-1} and cm^{-1}, respectively.

The single vibrational frequency of AsH has beeen determined by Anacona *et al.* [8] employing infrared laser spectroscopy. Moreover, the infrared spectra of AsH_3 (as well as PH_3 and SbH_3) were determined in solid argon by Arlinghaus and Andrews [9] and compared with earlier gas phase results. However, information on the fundamental frequencies of AsH_2 is lacking. In Table III are listed the normal vibrational modes for AsH and AsH_3 [8, 9]. In the case of AsH_2 estimated values are provided that are plausible in comparison with the known frequencies of the analogous hydride of phosphorus [10].

The symmetric stretch for AsH_2 was assigned between the observed stretching frequencies of AsH and AsH_3. A small bias was introduced in the direction of AsH because of the trend seen in the values reported for PH and PH_2 [10] in comparison with PH_3 [9]. The estimate for the antisymmetric stretch of AsH_2 is based on the fact that Arlinghaus and Andrews have found the antisymmetric mode to be 5–10 cm^{-1} higher than the symmetric one for both AsH_3 and PH_3 [9].

To estimate the bending frequency for AsH_2 use was made of stretching (k_1) and bending (k_d/l^2) force constants that can be obtained assuming simple valence forces. In the classic treatise of Herzberg on infrared and Raman spectra explicit formulae were been derived for the valence force constants of non-linear XY_2 and pyramidal XY_3 molecules [11]. The procedure adopted is as follows: (1) Evaluation of k_1 and k_d/l^2 as well as their ratio for AsH_3 from the normal vibrational modes (Table 3) and bond angle (Table 2). Since the equations are overdetermined

TABLE III Fundamental frequencies for AsH, AsH_2 and AsH_3 (cm^{-1})

Formula	Stretch	Bend	Antisymm. Stretch	Degeneracy	Antisymm. Bend	Degeneracy
AsH	2077					
AsH_2	2085	1060	2095	1		
AsH_3	2116	906	2123	2	1003	2

a pair of ratios $k_d/l^2/k_1$ were derived. (2) Calculation of $k_d/l^2/k_1$ for AsH_2 as a function of deformation frequency for fixed stretching vibrations (Table III). The estimated bending frequency AsH_2 is the frequency where the $k_d/l^2/k_1$ values for AsH_3 and AsH_2 overlap. Accordingly, the approximate bending frequency for AsH_2 is $960 \pm 20\ cm^{-1}$. When a similar procedure is applied to PH [12] and PH_3 [9], the estimated bending frequency becomes $1060 \pm 40\ cm^{-1}$ which is in reasonable accord with the reported value of $1102\ cm^{-1}$ [10].

At higher temperatures a small correction must be applied to the thermodynamic functions that reflects vibrational anharmonicity, centrifugal distortion, and vibration–rotation interaction. Employing appropriate formulae for diatomic molecules [6], the correction term can be readily evaluated for AsH from the molecular constants determined by Anacona *et al.* [8].

In Table I are listed the vibrational contributions to the entropy, *FEF*, enthalpy and heat capacity of AsH, AsH_2 and AsH_3 at 298, 1000, and 1500 K. In addition, also tabulated is the correction term to the thermodynamic functions of AsH on the line labelled 'anh'.

2.4. Electronic contribution

Excited electronic states of the gaseous molecules also contribute to the thermodynamic functions. To the best of our knowledge there is no information available on the electronic levels of As subhydrides. However, from estimated values for PH [2], we conclude that levels above the ground state will be negligible in the calculation of thermodynamic properties on account of the relatively high excitation energies ($\varepsilon \geq 7650\ cm^{-1}$). The ground state multiplicities, g, were assigned as 3, 2 and 1, respectively, for AsH, AsH_2 and AsH_3, in analogy with PH, PH_2 and NH_3 [2].

Taking into consideration only the ground state multiciplicity, the electronic contributions to the entropy, S_e° and free-energy function, FEF_e, become [6]

$$S_e^\circ = R \ln Q \tag{14}$$

and

$$FEF_e = -\left[\frac{(F^\circ - H_0^\circ)}{T}\right]_e = R \ln Q \tag{15}$$

where

$$Q = \sum_i g_i e^{-\varepsilon_i/kT} \equiv g$$

In Table I the temperature-independent S_e and FEF_e values are given for AsH and AsH_2.

2.5. Thermodynamic properties

Summing up the translational, vibrational rotational and electronic contributions to the thermodynamic properties of AsH, AsH_2 and AsH_3, one obtains the entropy, free energy function, enthalpy and heat capacity required for thermochemical calculations. The total standard property values for the three gaseous species are summarized in Table I.

In the case of gaseous AsH the main factors contributing to the thermodynamic functions are translation, rotation and the electronic ground state. The vibrational as well as the so-called correction term are almost negligible except at elevated temperatures. On the other hand, the vibrational contribution to the thermodynamic properties is more significant in the case of AsH_2 and AsH_3 on account of their more complex vibrational structure. Indeed, for AsH_3 the vibrational enthalpy ($H^\circ - H_0^\circ$) and heat capacity become larger than the rotational one as 1000 K is approached.

The data in Table I is in good accord with published compilations. The NBS Tables provide information on S°, $H^\circ - H_0^\circ$ and C_p° for AsH_3 but only at 298 K [3]. The respective values of $53.25\ cal\ mol^{-1}\ deg^{-1}$, $2438\ cal\ mol^{-1}$, and $9.09\ cal\ mol^{-1}\ deg^{-1}$ are in excellent agreement with the results given in Table I. Moreover, the absolute entropies for AsH and AsH_2 at 298 K of 49.741 and 53.821 $cal\ mol^{-1}\ deg^{-1}$, respectively, are reasonable in comparison with that for PH ($46.9\ cal\ mol^{-1}\ deg^{-1}$) and PH_2 ($50.8\ cal\ mol\ deg^{-1}$) [2]. Here, the difference between the S° of As and P-subhydrides is consistent with that for AsH_3 ($53.252\ cal\ mol^{-1}\ deg^{-1}$) and PH_3 ($50.293\ cal\ mol^{-1}\ deg$) which mainly reflects the difference in the atomic weight of the group V elements.

3. Results and applications

In this section complete thermodynamic Tables for gaseous AsH, AsH_2 and AsH_3 are provided. Furthermore, the enthalpies of formation for the three species are evalulated from bond energy data. Finally, the data is applied to the temperature-dependent decomposition of AsH_3 and examples provided of experimental verification.

3.1. Thermodynamic tables

In Tables IV, are presented the standard entropy, *FEF*, enthalpy and heat capacity for AsH, AsH_2 and AsH_3 up to 1600 K, in 100 K intervals. In accord with the usual convention the *FEF* and enthalpy are referred to 298 K [6]. Here, the *FEF* is defined as

$$FEF = -(F^\circ - H_{298}^\circ)/T \tag{16}$$

which should be compared with the original expression in Equation 2

$$FEF' = -(F^\circ - H_0^\circ)/T$$

Clearly, the *FEF* in Equation 16 can be obtained from the values in Table 1 (*FEF'*) according to

$$FEF = FEF' + \frac{(H_{298}^\circ - H_0^\circ)}{T} \quad (17)$$

where the numerator of the second term is given in Table I.

The enthalpy referred to 298 K is

$$H^\circ - H_{298}^\circ = H^\circ - H_0^\circ - (H_{298}^\circ - H_0^\circ) \quad (18)$$

where first and second terms are enthalpy values from Table 1. Thus the tabulated enthalpy at 298 K is always zero.

3.2. Enthalpies of formation of hydrides

In order to perform any calculations involving chemical equilibria, the tabulated thermodynamic functions must be complemented with the enthalpy of formation of the gaseous hydrides. In a recent photoionization mass spectrometric study of AsH, AsH_2, and AsH_3, Berkowitz determined the bond energies for the three hydrides [5]. The bond energies can be represented by the following chemical equilibria:

$$As(g) + H(g) = AsH(g) - 64.6\,\text{kcal} \quad (19)$$

$$AsH(g) + H(g) = AsH_2(g) - 66.5\,\text{kcal} \quad (20)$$

$$AsH_2(g) + H(g) = AsH_3(g) - 74.9\,\text{kcal} \quad (21)$$

The enthalpies of formaton at 0, $\Delta H_f^\circ(0\,K)$ are related to the above bond energies via a thermochemical

TABLE IV Thermodynamic tables for $AsH(g)$, $AsH_2(g)$ and $AsH_3(g)$

TABLE IV.1

$AsH(g)$

T (K)	$-[F^\circ - H_{298}^\circ]/T$ (cal mol^{-1} deg^{-1})	S° (cal mol^{-1} deg^{-1})	$H^\circ - H_{298}^\circ$ (cal mol)	C_p° (cal mol^{-1} deg^{-1})
0	infinite	0	− 2068.7	0
100	55.933	42.135	− 1379.9	6.959
200	50.379	46.959	− 683.8	6.963
298	49.741	49.741	0	6.975
300	49.741	49.784	12.9	6.976
400	50.015	51.798	712.9	7.035
500	50.535	53.380	1422.1	7.160
600	51.122	54.700	2146.5	7.332
700	51.717	55.844	2889.1	7.522
800	52.298	56.861	3650.8	7.709
900	52.856	57.779	4430.4	7.881
1000	53.391	58.618	5226.4	8.036
1100	53.902	59.390	6036.9	8.172
1200	54.390	60.106	6860.2	8.291
1300	54.855	60.774	7694.7	8.395
1400	55.301	61.400	8538.9	8.487
1500	55.727	61.988	9391.6	8.567
1600	56.136	62.543	10252.0	8.639

TABLE IV.2

AsH_2

T (K)	$-[F^\circ - H_{298}^\circ]/T$ (cal mol^{-1} deg^{-1})	S° (cal mol^{-1} deg^{-1})	$H^\circ - H_{298}^\circ$ (cal mol^{-1})	C_p° (cal mol^{-1} deg^{-1})
0	infinite	0	− 2397.5	0
100	61.052	45.026	− 1602.6	7.949
200	54.576	50.552	− 804.9	8.044
298	53.822	53.821	0	8.389
300	53.822	53.873	15.5	8.397
400	54.156	56.352	878.3	8.871
500	54.805	58.387	1791.3	9.392
600	55.552	60.147	2757.1	9.923
700	56.322	61.715	3774.9	10.426
800	57.086	63.137	4840.6	10.879
900	57.832	64.442	5948.8	11.275
1000	58.554	65.648	7093.6	11.613
1100	59.251	66.768	8269.8	11.901
1200	59.921	67.815	9472.4	12.144
1300	60.567	68.795	10697.4	12.350
1400	61.187	69.717	11941.4	12.525
1500	61.785	70.586	13201.5	12.674
1600	62.361	71.408	14475.5	12.802

TABLE IV.3
$AsH_3(g)$

T (K)	$-[F^\circ - H^\circ_{298}]/T$ (cal mol^{-1} deg^{-1})	S° (cal mol^{-1} deg^{-1})	$H^\circ - H^\circ_{298}$ (cal mol^{-1})	C°_p (cal mol^{-1} deg^{-1})
0	infinite	0	− 2449.5	0
100	60.791	44.249	− 1654.6	7.950
200	54.059	49.801	− 851.6	8.227
298	53.252	53.252	0	9.211
300	53.252	53.309	17.1	9.234
400	53.629	56.135	1002.4	10.477
500	54.382	58.604	2110.9	11.681
600	55.274	60.833	3335.1	12.782
700	56.216	62.878	4663.2	13.758
800	57.169	64.772	6082.3	14.601
900	58.113	66.534	7579.3	15.318
1000	59.038	68.180	9142.1	15.921
1100	59.940	69.722	10760.2	16.427
1200	60.816	71.170	12424.8	16.852
1300	61.666	72.533	14128.3	17.209
1400	62.488	73.820	15864.8	17.511
1500	63.285	75.037	17629.1	17.768
1600	64.056	76.191	19417.1	17.987

cycle and given by the enthalpies of reaction for

$$As(s) + \tfrac{1}{2}H_2(g) = AsH(g) \quad (22)$$

$$As(s) + H_2(g) = AsH_2(g) \quad (23)$$

and

$$As(s) + \tfrac{3}{2}H_2(g) = AsH_3(g) \quad (24)$$

The evaluation of $\Delta H^\circ_f(0\ K)$ will only be illustrated for Equation 22 since the method is readily applicable to Equations 23 and 24. Reaction 22 is equivalent to the following cycle

$$As(g) + H(g) = AsH(g) \quad (22a)$$

$$\tfrac{1}{2}H_2(g) = H(g) \quad (22b)$$

$$As(s) = \tfrac{1}{4}As_4(g) \quad (22c)$$

$$\tfrac{1}{4}As_4(g) = \tfrac{1}{2}As_2(g) \quad (22d)$$

$$\tfrac{1}{2}As_2(g) = As(g) \quad (22e)$$

Clearly, Equation 22a is the bond energy value of Berkowitz (Equation 19; [5]) the enthalpy values for reactions 22b and 22d were taken from the JANAF Tables [2] and Murray *et al.* [13], respectively. An exhaustive assessment of the relevant sources of enthalpy data including reaction 22e has been given by Berkowitz [5]. In Table V are summarized the enthalpies of formation for the three hydrides at 0 and 298 K.

To obtain $\Delta H^\circ_f(298)$ for reaction 22 the thermodynamic relationship

$$\Delta H^\circ_f(298) = \Delta H^\circ_f(0) + (H^\circ_{298} - H^\circ_0)_{AsH(g)} - (H^\circ_{298} - H^\circ_0)_{As(s)} - \tfrac{1}{2}(H^\circ_{298} - H^\circ_0)_{H_2(g)} \quad (25)$$

was employed.

The required enthalpy values in Equation 25 for $AsH(g)$, $As(s)$, and $H_2(g)$, respectively, are given in Table III, Stull and Sinke [14] and JANAF [2]. Expressions analogous to Equation 25 can be readily evaluated for $AsH_2(g)$ and $AsH_3(g)$.

TABLE V Enthalpies of formation of As hydrides

Species	$\Delta H^\circ_f(0)$ (kcal)	$\Delta H^\circ_f(298)$ (kcal)
AsH	55.81	55.64
AsH_2	40.94	40.09
AsH_3	17.67	15.86

3.3. Application to the decomposition of AsH_3

The decomposition of AsH_3 to various gaseous species is of widespread interest to the III–V epitaxial growth community. AsH_3 is the commonly used As source in low-pressure MOCVD (LP-MOCVD), atmospheric-pressure MOCVD (AP-MOCVD), HS-MBE [15] and MOMBE [16]. In the MBE-based techniques a hydride cracker is employed [17]. In this section the equilibrium composition of gas phase for a fixed AsH_3 input is determined as a function of temperature at the total pressures (p_{tot}) of 1.013, 3.039×10^3 and 1.013×10^5 Pa, corresponding approximately to MOMBE (HS-MBE), LP-MOCVD, and AP-MOCVD conditions, respectively.

The gaseous species under consideration are As, As_2, As_4, AsH, AsH_2, AsH_3, H and H_2. In a thermodynamic sense, the system is completely described by the six reactions 19, 20, 21, 22b, 22d and 22e. In principle, the gas phase composition can be calculated at a constant T and p_{tot} from the six equilibrium constants and the number of moles of AsH_3 in the input, using six 'extent of reaction' independent variables. Thermodynamic data in the literature [2, 14, 18] complemented by the *FEF*s and ΔH°_fs in Tables IV and V for the As-hydrides permit the evaluation of

the equilibrium constants. However, the resulting non-linear algebraic equations presented serious numerical difficulties when using a standard 'solver' program. In particular, the gas-phase compositions did not converge and were very sensitive to the initial estimate.

Consequently, a free-energy minimizaton technique [19] was adopted which will be described in more detail in a forthcoming paper [20]. Here the procedure is only briefly outlined. Accordingly, for each of the species the Gibbs free energy ($F°$) is determined as a function of T from the relationship

$$F° = -(FEF)T + \Delta H_f°(298)$$

$$= T\frac{(F° - H°_{298})}{T} + \Delta H_f°(298) \qquad (26)$$

where the enthalpy terms cancel because the enthalpy of elements in their standard states at 298 K is by definition equal to zero. The free energy functions and $\Delta H_f°$s are listed in Tables IV and V, respectively, for the As-hydrides; the relevant data for As, As_2 [14], As_4 [18], H and H_2 [2] can be obtained from the literature.

Subsequently, for each species the chemical potential is evaluated in the ideal gas state. The closed system is constrained by mass balance (input AsH_3). Next, the total free energy of the system is minimized and the constraint is removed by Lagrange multipliers [19]. Finally, in the present problem a system of two algebraic equations in the Lagrange multipliers is obtained which can be solved by the Newton–Raphson iteration technique. The resulting concentrations are robust and independent of the starting values for the multipliers.

In Fig. 1 we present the mole fractions of the various species, resulting from the decomposition of AsH_3, as a functon of temperature at $p_{tot} = 1.013$ Pa. This pressure is of particular interest in the operation of an AsH_3 cracker employed in HS-MBE and MOMBE, especially in the temperature range between 1000 and 1300 K. The partial pressures of the major species, As_2 and H_2, are nearly independent of temperature while the partial pressure of As_4 rapidly decreases as the temperature rises. Huet *et al.* [21] determined the relative amounts of As_2 and As_4 in a cracker cell employed in HS-MBE growth experiments by a modulated beam mass spectrometric technique. At 1000 °C the observed dimer-tetramer ratio is ≈ 1000 which is comparable with the equilibrium value of ≈ 1300, if allowance is made for the enrichment of the cracker with As_2 at the expense of H_2 under effusive flow conditions. One should be aware of the fact that the equilibrium calculations are sensitive to both the *FEF*s and the enthalpies of formation (ΔH_f^0 (298)). In particular, adding only 2 kcal at 298 K to the enthalpy of the dissociation reaction $As_4 = 2\,As_2$ yields dimer–tetramer ratios that are about a factor of 2 lower.

There is also a rapid $\approx$ 30-fold rise in the mole fraction of monatomic As and H. At 1300 K the monatomic H partial pressure is $\approx 3.33 \times 10^{-4}$ Pa at the cracker which translates to 3.33×10^{-6} Pa beam equivalent pressure at the surface of the wafer. The partial

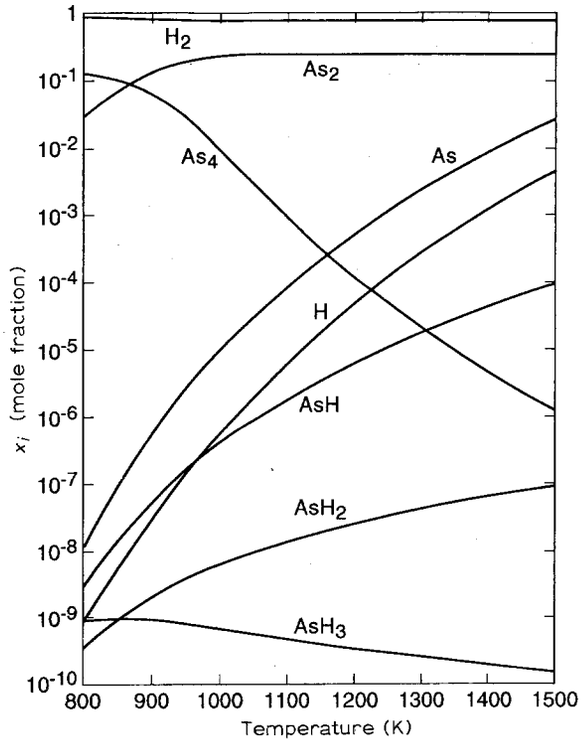

Figure 1 The equilibrium composition of the gas phase as a function of temperature during the pyrolysis of AsH_3. The total pressure (p_{tot}) is 1.013 Pa and the concentrations are given in mole fractions (x_i). The product $x_i p_{tot}$ provides the species partial pressures.

pressure of As is about an order of magnitude higher. The most prominent subhydride is AsH producing a partial pressure of 1.87×10^{-5} Pa at the exit of the cracker operating at 1300 K. Consequently, in thermodynamic equilibrium H and AsH are predicted to be the most important species in the removal of carbon-containing radicals [22] and oxygen.

In Fig. 2, is displayed the temperature dependence of the various species in thermodynamic equilibrium arising from the decomposition of AsH_3 at $p_{tot} = 3.039 \times 10^3$ Pa, a pressure frequently employed in LP-MOCVD applications. In the characteristic temperature range of 800–1100 K the most prominent feature in Fig. 2 is the large drop in the tetramer-to-dimer ratio of As (p_{As_4}/p_{As_2}). Since the sticking coefficients of As_4 and As_2 on a Ga-stabilized GaAs surface are respectively, 0.5 and 1 [23], at a constant AsH_3 pressure, higher growth temperatures produce a vapour phase containing a larger effective flux of arsenic.

In the case of quaternary growth of InGaAsP, a major concern is the manner in which p_{P_4}/p_{P_2} tracks p_{As_4}/p_{As_2}. At the deposition temperature for quaternary films (≈ 650 °C) there is a significant amount of dimers in the gas phase, especially when AsH_3 and PH_3 are heavily diluted with H_2. As the temperature rises the tetramer–dimer lines intersect and above a 'cross-over' temperature dimers become the majority species instead of the tetramers. The more closely matched are the atomic H/As and H/P ratios, the less is the separation between the cross-over temperatures for p_{P_4}/p_{P_2} and p_{As_4}/p_{As_2} and thus the As and P partial pressures track each other.

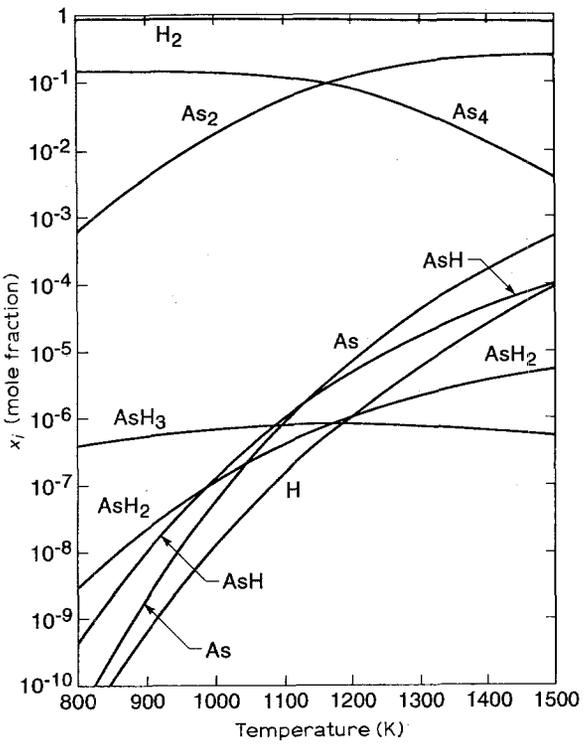

Figure 2 The equilibrium composition of the gas phase as a function of temperature during the pyrolysis of AsH_3. The total pressure (p_{tot}) is 3.039×10^3 Pa and the concentrations are given in mole fractions (x_i). The product $x_i p_{tot}$ provides the species partial pressures.

Zilko *et al.* [24] have recently noticed that the compositional uniformity of group V sites in 1.3 μm quaternary material improved as they changed from the source combination AsH_3 and PH_3 to TBAs (tertiary butyl arsine) and TBP and then to AsH_3 and TBP. Detailed thermodynamic calculations including H_2 dilution indicate that the separation in cross-over temperatures is reduced from 75 to 50 and then to 25 °C for the same source sequence. To provide a more definitive thermodynamic interpretation of the compositional uniformity data, we have examined the [As/P] ratio in the gas phase as a function of reciprocal T and demonstrated that in the MOCVD range (900–950 K) the slope of these curves changes from steep to moderate and then nearly flat for the sources $AsH_3 + PH_3$, TBAs + TBP, and AsH_3 + TBP, respectively [25]. The insensitivity of the [As/P] ratio to the ≈ 30 K gradient over the susceptor when combining AsH_3 and TBP suggests a very effective method to assure compositional uniformity in qaternary layers prepared by LP-MOCVD.

Obviously, the thermodynamic results in Fig. 2 show that the dissociation of AsH_3 is less complete at 3.039×10^3 than at 1.013 Pa. With regard to subhydrides, at 1000 K AsH and AsH_2 are equally important providing a partial pressure of 2.67×10^{-4} Pa. Under the same conditions the atomic H pressure is an order of magnitude lower. Therefore, in comparing AP-MOCVD or LP-MOCVD and MOMBE, the removal of alkyl radical species is expected to be enhanced by the subhydrides (AsH + AsH_2) and H, respectively, at the growth front. For LP-MOCVD the combined subhydride partial pressure is 5.332×10^{-4} Pa, while for MOMBE the beam equivalent H pressure is 3.33×10^{-6} Pa ($\sim p_H/100$). This factor may explain the relatively higher purity and thus the lower carbon contamination achievable to date in MOCVD than in MOMBE.

In Fig. 3 are plotted the mole fractions of the decomposition products of AsH_3 versus temperature at $p_{tot} = 1.013 \times 10^5$ Pa. The temperature range 800–1100 K is relevant to AP-MOCVD. In this case the dominant As-bearing species is As_4 and the p_{As_4}/p_{As_2} ratio drops from ≈ 1000 to ~ 40 between 800 and 1000 K. We have compared the equilibrium dimer and tetramer partial pressures with the mass spectrometric results of Ban [26] at 850 °C and found the calculated values of p_{As_2} and p_{As_4} to be wthin a factor of 0.7 and 1.5, respectively. Whether this difference is due to an artifact in the experimental technique (a capillary tube connected to the spectrometer samples the products of pyrolysis in a horizontal reactor) or to a kinetic limitation of the dimer to tetramer association reaction (i.e. $2As_2 = As_4$) is difficult to ascertain. In any case under atmospheric pressure conditions the tetramers are the major species which serves as the likely explanation for the excellent compositional uniformity on the group V sites in InGaAsP layers grown by AP-MOCVD employing AsH_3 and PH_3 [27]. At 1000 K, the species that are predicted to be active in removing alkyl radicals from the growth interface in decreasing order of importance are AsH_2, AsH and H, having partial pressures

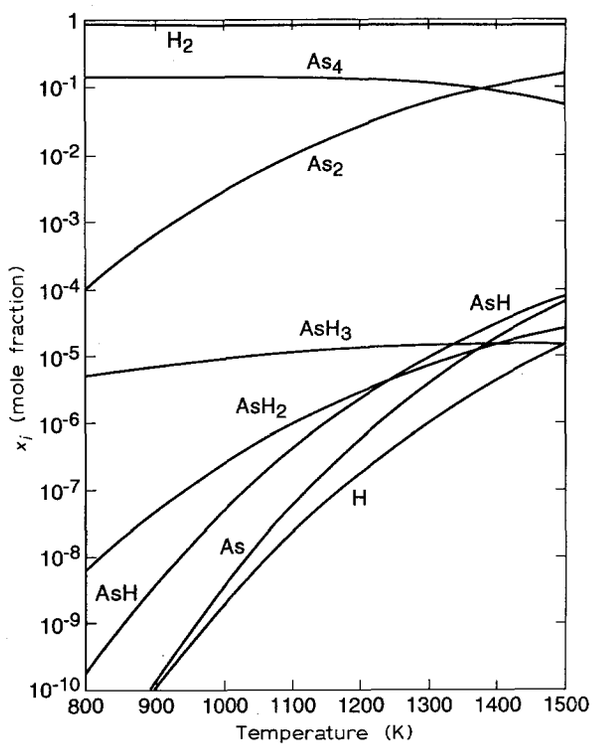

Figure 3 The equilibrium composition of the gas phase as a function of temperature during the pyrolysis of AsH_3. The total pressure (p_{tot}) is 1.013 × 10^5 Pa and the concentrations are given in mole fractions (x_i). The product $x_i p_{tot}$ provides the species partial pressures.

of $\approx 3.33 \times 10^{-2}$, 5.33×10^{-3}, and 2.0×10^{-4} Pa, respectively. The presence of PH_2 and AsH_2 has been identified by Raman spectroscopy during PH_3 and AsH_3 pyrolysis in an AP-MOCVD reactor [28].

References

1. G. B. STRINGFELLOW, "Organometallic Vapor-Phase Epitaxy: Theory and Practice" (Academic Press, San Diego, CA, 1989).
2. D. R. STULL and H. PROPHET, "JANAF Thermochemical Tables" 2nd Edn, (National Bureau of Standards, Washington, DC, 1971).
3. D. D. WAGMAN, W. H. EVANS, V. B. PARKER, R. H. SCHUMM, I. HALOW, S. M. BAILEY, K. L. CHURNEY and R. L. NUTTAL, "The NBS Tables of Chemical Thermodynamic Properties" (American Chemical Society and American Institute of Physics, New York, 1982).
4. M. TIRTOWIDJOJO and R. POLLARD, *J. Cryst. Growth* **77** (1986) 200.
5. J. BERKOWITZ, *J. Chem. Phys.* **89** (1988) 7065.
6. G. N. LEWIS and M. RANDALL, Revised by K. S. Pitzer and L. Brewer, "Thermodynamics", 2nd Edn, (McGraw-Hill, New York, 1961).
7. D. DAI and K. BALASUBRAMANIAN, *J. Chem. Phys.* **93** (1990) 1837.
8. J. R. ANACONA, P. B. DAVIES and S. A. JOHNSON, *Mol. Phys.* **56** (1985) 989.
9. R. T. ARLINGHAUS and L. ANDREWS, *J. Chem. Phys.* **81** (1984) 4341.
10. M. E. JACOX, *J. Phys. Chem. Ref. Data* **13** (1984) 945.
11. G. HERZBERG, "Molecular Spectra and Molecular Structure. II Infrared and Raman Spectra of Polyatomic Molecules" (D. Van Nostrand, Princeton, NJ, 1968).
12. J. R. ANACONA, P. B. DAVIES and P. A. HAMILTON, *Chem. Phys. Lett.* **104** (1984) 269.
13. J. J. MURRAY, C. PUPP and R. F. POTTIE, *J. Chem. Phys.* **58** (1973) 2569.
14. D. R. STULL and G. C. SINKE, "Thermodynamic Properties of the Elements" Advances in Chemistry Series No. 18 (American Chemical Society, Washington, 1956).
15. M. B. PANISH, *J. Cryst. Growth* **81** (1987) 249.
16. W. T. TSANG, *ibid.* **81** (1987) 261.
17. M. B. PANISH and H. TEMKIN, *Annu. Rev. Mater. Sci.* **19** (1989) 209.
18. R. J. CAPWELL, Jr. and G. M. ROSENBLATT, *J. Mol. Spectrosc.* **33** (1970) 525.
19. W. R. SMITH and R. W. MISSEN, "Chemical Reaction Equilibrium Analysis: Theory and Algorithms" (John Wiley and Sons, New York, 1982).
20. A. S. JORDAN and A. ROBERTSON, submitted to *J. Vac. Sci. Technol.* **B.**
21. D. HUET, M. LAMBERT, D. BONNERIE and D. DUFRESNE, *J. Vac. Sci. Technol.* **B3** (1985) 823.
22. See page 262 of Reference 1
23. C. T. FOXON and B. A. JOYCE, *Surf. Sci.* **64** (1977) 293; **50** (1975) 434.
24. J. L. ZILKO, P. S. DAVISSON, L. LUTHER and K. D. C. TRAPP, *J. Cryst. Growth* **124** (1992) 112.
25. A. S. JORDAN, A. ROBERTSON and J. L. ZILKO, *Appl. Phys. Lett.* **62** (1993) 360.
26. V. S. BAN, *J. Electrochem. Soc.* **118** (1971) 1473.
27. A. W. NELSON, P. C. SPURDENS, S. COLE, R. H. WALLING, R. H. MOSS, S. WONG, M. J. HARDING, D. M. COOPER, W. J. DEVLIN and M. J. ROBERTSON, *J. Cryst. Growth* **93** (1988) 792.
28. P. ABRAHAM, A. BEKKAOUI, V. SOULIERE, J. BOUIX and Y. MONTEIL, *ibid.* **107** (1991) 26.

Received 15 June
and accepted 5 October 1992